

Electronic Supporting Information (ESI)

## Cyclodextrin-Derived Polymer Networks for Selective Molecular Adsorption

Bailey Phillips,<sup>a</sup> Chenxu Wang,<sup>b</sup> Xinman Tu,<sup>c\*</sup> Che-Hsuan Chang,<sup>a</sup> Sarbajit Banerjee,<sup>a,b</sup>  
Mohammed Al-Hashimi,<sup>d</sup> Wei Hu,<sup>e\*</sup> and Lei Fang<sup>a,b\*</sup>

<sup>a</sup> Department of Chemistry, <sup>b</sup> Department of Materials Science and Engineering, Texas A&M University, College Station, Texas 77843, United States

<sup>c</sup> Key Laboratory of Jiangxi Province for Persistent Pollutants Control and Resources Recycle, College of Environmental and Chemical Engineering, Nanchang Hangkong University, Nanchang 330063, China.

<sup>d</sup> Department of Chemistry, Texas A&M University at Qatar, P.O. Box 23874, Doha, Qatar

<sup>e</sup> Department of Electronic Engineering, Tsinghua University, Beijing 100084, China

### Supporting Information

*Correspondence Address
Professor Xinman Tu Key Laboratory of Jiangxi Province for Persistent Pollutants Control and Resources Recycle, College of Environmental and Chemical Engineering, Nanchang Hangkong University, Nanchang 330063, China tuxinman@126.com
Professor Wei Hu Department of Electronic Engineering Tsinghua University, Beijing 100084, China weihu@mail.tsinghua.edu.cn
Professor Lei Fang Department of Chemistry, Texas A&M University, 3255 TAMU College Station, TX 77845-3255, USA Tel: +1 (979) 845 3186 E-Mail: fang@chem.tamu.edu

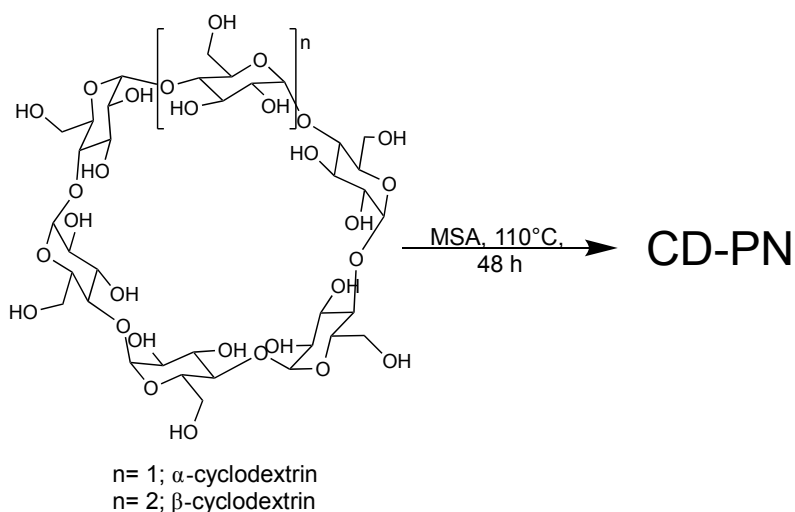
# Table of Contents

1. General Method.....	3
2. Synthetic Procedures.....	3
3. X-Ray Photoelectron Spectroscopy.....	5
4. Solid-State NMR.....	6
5. Fourier Transform Infrared Spectroscopy.....	7
6. Thermogravimetric Analysis.....	9
7. Elemental Analysis Calculation.....	10
8. Film Fabrication.....	10
9. Scanning Electron Microscopy.....	11
10. Structure Size Modeling.....	12
11. Adsorption Performance.....	13
12. Cyclodextrin-Based Polymer Comparison.....	18

## 1. General Method

All starting materials and solvents were obtained from commercial suppliers and used without further purification. Activated charcoal was purchased from Sigma-Aldrich with a 100-mesh particle size for adsorption tests. X-ray photoelectron spectroscopy (XPS) data were obtained using an Omicron XPS/UPS system with Argus detector. Solid-state NMR spectra were obtained on a Bruker Avance 400 MHz spectrometer at magic angle spinning (MAS) rates of 10 kHz with 4 mm CP/MAS probes at room temperature. Fourier transform infrared (FTIR) Spectroscopy was recorded using a Shimadzu IRAffinity-1S spectrometer. UV-visible absorption spectra were recorded on a Shimadzu UV-2600 UV-Vis Spectrophotometer. Field-emission scanning electron microscopic (SEM) images were collected using a JEOL JSM-7500F FE-SEM at 5 kV. Samples were sputter coated in platinum/palladium prior to imaging. Thermogravimetric analysis (TGA) was carried out with a TA Q500 thermogravimetric analyzer at a heating rate of 20°C min<sup>-1</sup> from 30°C to 900°C under N<sub>2</sub> atmosphere. Elemental analysis was performed by Robertson Microlit Laboratories for elemental CHN analysis.

## 2. Synthetic Procedures

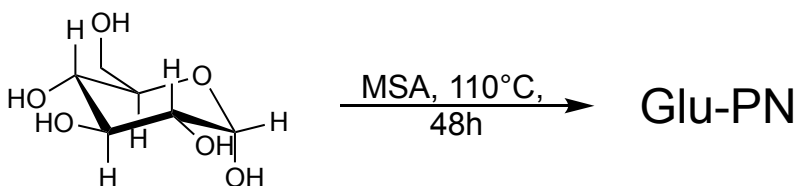


**Scheme S1.** Synthesis of α- and β-CD-PN via methanesulfonic acid-mediated condensation.

**$\alpha$ -CD-PN and  $\beta$ -CD-PN:** Cyclodextrin, either  $\beta$  or  $\alpha$ , (15.0 g, 13.2 mmol if  $\beta$ -CD or 5.0 g, 5.1 mmol if  $\alpha$ -CD) was dissolved in methanesulfonic acid (150 mL) and pre-reacted for 45 minutes with bath sonication to form a dark red solution. The solution was then heated and maintained at 110°C for 48 h. Afterwards, the solution was cooled in an ice bath and quenched with water. The solid was collected and washed with copious amounts of water. Soxhlet extraction by water was then conducted for 24 h to remove uncross-linked low molecular weight material. Subsequently, the solid was dried in a vacuum oven at 80°C for 24 h. The dried solid,  **$\alpha$ -CD-PN (3.4 g, 68 % yield)** and  **$\beta$ -CD-PN (9.6 g, 64 % yield)** was then ground into a fine powder with a coffee grinder for further characterization and performance tests.

Percent yield based on cyclodextrin monomer mass is defined by *Equation S1*. The number of moles of water lost during the reaction can be estimated from the percent yield based on the assumption that all weight loss is due to water loss. Using this method, it is estimated that 22.69 mol of H<sub>2</sub>O are lost per mole of  $\beta$ -cyclodextrin monomer and 17.43 mol of H<sub>2</sub>O are lost per mole of  $\alpha$ -cyclodextrin monomer.

$$\% \text{ yield} = \left( \frac{\text{mass of isolated CD - PN}}{\text{mass of CD monomer}} \times 100 \right) \quad (\text{Equation S1})$$



**Scheme S2.** Synthesis of **Glu-PN** via methanesulfonic acid-mediated condensation.

**Glucose-Derived Polymer Network (Glu-PN):** d-(+)-Glucose (5.0 g, 27.7 mmol) was dissolved in methanesulfonic acid (50 mL) and pre-reacted for 45 minutes under bath sonication. The

solution was then heated and maintained at 110°C for 48 h. Afterwards, the solution was cooled in an ice bath and quenched with water. The solid was collected and washed with copious amounts of water. Soxhlet extraction by water was then conducted for 24 h to remove uncross-linked low molecular weight material. Subsequently, the solid was dried in a vacuum oven at 80°C for 24 h. The dried solid, **Glu-PN (4.3 g, 86 % yield)** was then ground into a fine powder with a coffee grinder for further characterization and performance tests.

### 3. X-Ray Photoelectron Spectroscopy

In order to monitor how the reaction temperature impacts the level of dehydration in the product, three batches of **β-CD-PN** were synthesized with the reaction temperature varied at 50°C, 80°C, and 110°C. XPS was used to analyze the nature of carbon in the material. The shift of the C1s C—C peak towards 284 eV corresponding to  $sp^2$  carbon indicated that dehydration via acid-mediated elimination occurred along with cross-linking during the reaction. The content of  $sp^2$  carbon increased as the temperature was elevated as evidenced by a consistent shift of the C1s C—C peak towards 284 eV (**Fig. S2**).

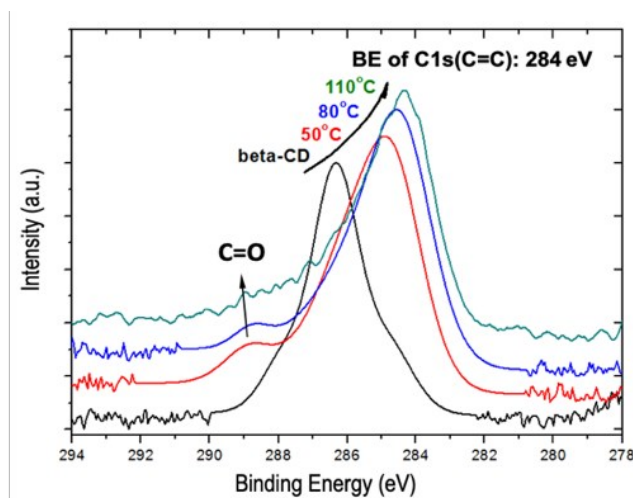


**Fig. S1** Correlation between the reaction temperature and C1s XPS peak of  $\beta$ -CD and  $\beta$ -CD-PN prepared under varying temperatures.

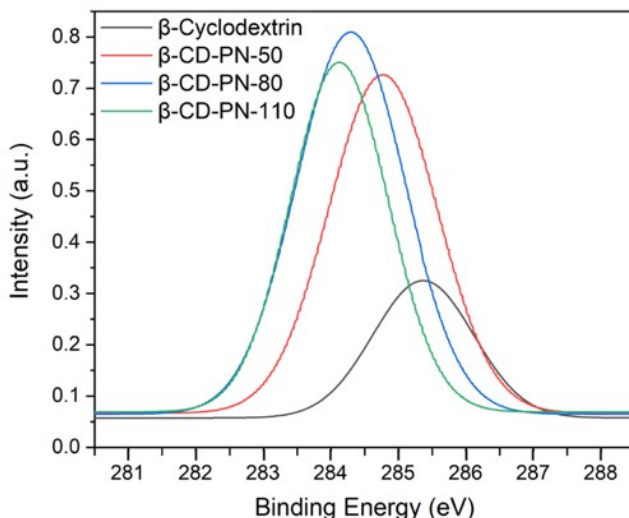


**Fig. S2** XPS C1s C—C deconvoluted peaks of  $\beta$ -CD and  $\beta$ -CD-PN prepared under varying temperatures.

**Table S1.** Table of XPS C1s peak positions and areas for  $\beta$ -CD and  $\beta$ -CD-PN prepared under varying temperatures.

Peak	$\beta$ -CD		$\beta$ -CD-PN 50°C		$\beta$ -CD-PN 80°C		$\beta$ -CD-PN 110°C	
	Position	Peak Area	Position	Peak Area	Position	Peak Area	Position	Peak Area
C—C	284.7	17.92	284.6	48.00	284.4	58.30	284.1	49.30
C—O	286.3	68.89	285.9	44.18	285.7	38.10	285.5	39.50
C=O	287.9	12.19	288.9	7.83	288.8	3.60	288.1	11.20

#### 4. Solid-State NMR

Solid-state  $^{13}\text{C}$  CP/MAS NMR of  $\beta$ -CD-PN and  $\beta$ -cyclodextrin were measured at room temperature in the powder form. In the  $\beta$ -CD-PN spectrum, the emergence of peaks ranging from  $\sim 180 - 215$  ppm indicate the presence of carbonyls within the polymer, which is not observed in

$\beta$ -cyclodextrin (**Fig. S3**). Additionally, a peak around 155 ppm indicates the presence of alkene  $sp^2$  carbons in  $\beta$ -CD-PN as observed in XPS (**Fig. S2**).

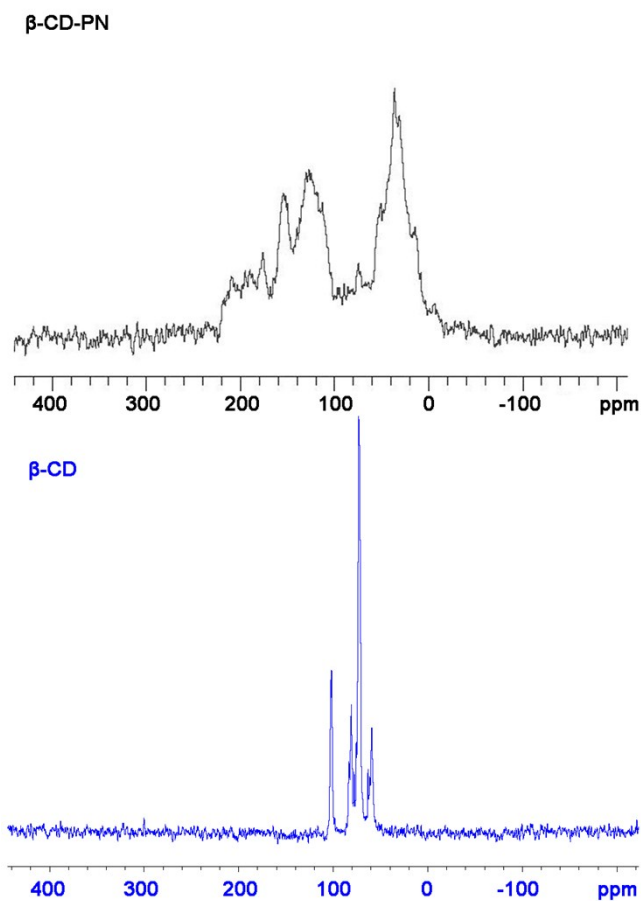


**Fig. S3** Solid-state CP/MAS  $^{13}\text{C}$  NMR spectra of  $\beta$ -CD-PN and  $\beta$ -cyclodextrin.

## 5. Fourier Transform Infrared Spectroscopy

FTIR spectra and table of peak assignments is shown below for  $\beta$ -CD-PN and  $\beta$ -cyclodextrin. The emergence of peaks indicative of  $sp^2$  carbons are consistent with the dehydration observed from NMR and XPS (**Fig. S2** and **S3**). Additionally, the FTIR spectra of  $\beta$ -CD-PN and  $\beta$ -CD-PN-Film are compared in **Fig. S4** demonstrating that the structure and functional groups of the bulk powder material and the thin film are the same.

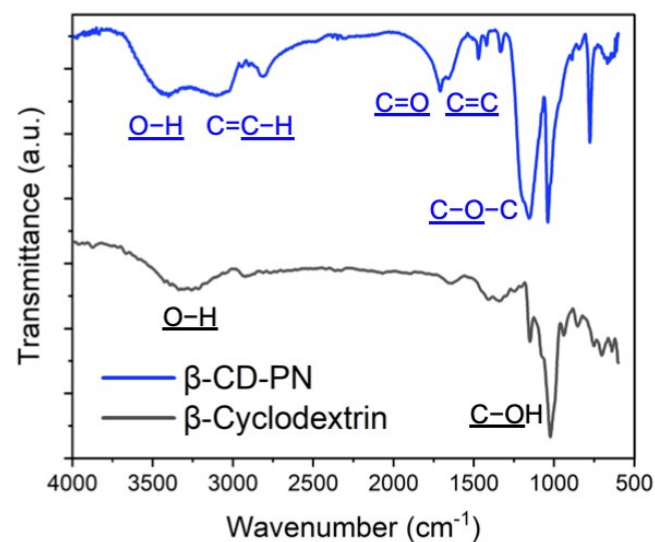


**Fig.S4** FTIR spectra of  $\beta$ -CD-PN compared with  $\beta$ -cyclodextrin starting material.

**Table S2.** FTIR peak assignments of  $\beta$ -CD-PN and  $\beta$ -cyclodextrin.

	$\beta$ -CD-PN	$\beta$ -Cyclodextrin
Functional Group	Absorption ( $\text{cm}^{-1}$ )	Absorption ( $\text{cm}^{-1}$ )
<u>C-O-H</u>	1039	1024
<u>C-O-C</u>	1157	1151
<u>C=C</u>	1658	—
<u>C=O</u>	1710	—
<u>C=C-H</u>	3101	—
<u>O-H</u>	3400	3336

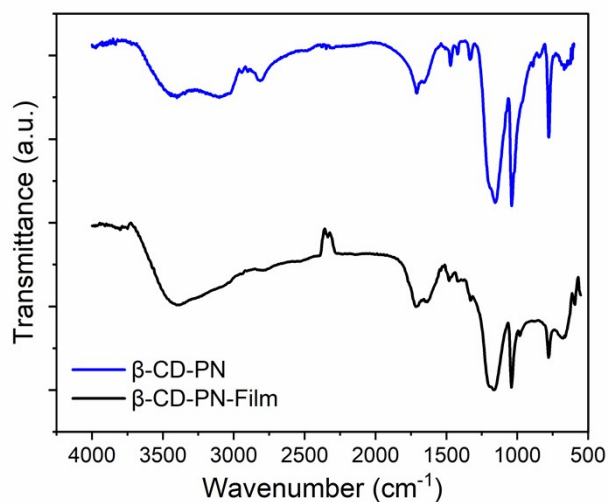


**Fig. S5** FTIR spectra comparison of  $\beta$ -CD-PN and  $\beta$ -CD-PN-Film.

## 6. Thermogravimetric Analysis

Thermogravimetric analysis (TGA) of  $\beta$ -CD-PN and  $\beta$ -cyclodextrin starting material are shown below. TGA was conducted in a  $N_2$  atmosphere. The dehydration of  $\beta$ -CD-PN leads to an enhanced carbonization yield of  $\beta$ -CD-PN (47%) compared with the  $\beta$ -cyclodextrin starting material (14%).

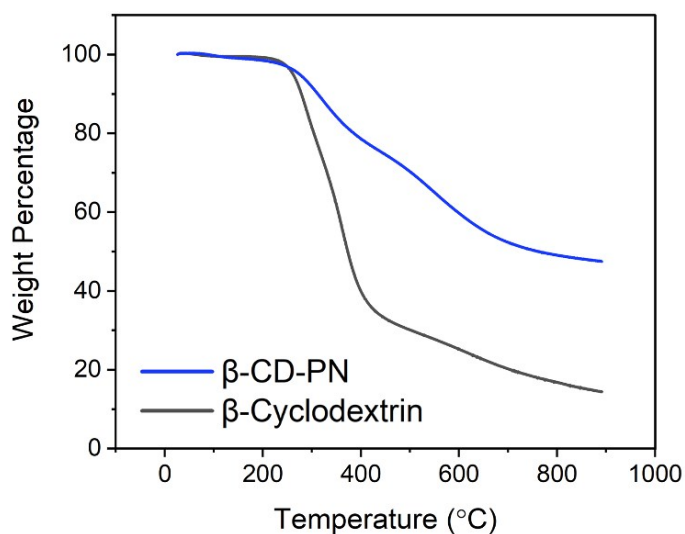
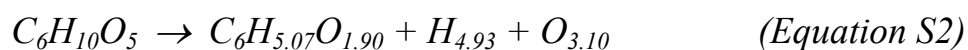


**Fig. S6** TGA plot of  $\beta$ -CD-PN compared with  $\beta$ -cyclodextrin starting material in  $N_2$  atmosphere.

## 7. Elemental Analysis Calculation

The extent of dehydration was estimated based on elemental analysis data from  $\beta$ -CD-PN and  $\beta$ -cyclodextrin. The empirical formula of  $\beta$ -CD-PN was determined based on the elemental analysis results, while the degree of dehydration was estimated based on the assumption of no carbon loss during the reaction. Using the respective empirical formulas, the amount of hydrogen and oxygen lost was determined and listed in *Equation S2*.



The extent of hydrogen and oxygen lost was averaged to give an estimation of  $\sim 2.78$  moles of water lost per glucopyranosidic unit, *i.e.*,  $\sim 19.46$  moles of water lost per mole of  $\beta$ -cyclodextrin.

## 8. Film Fabrication

**$\beta$ -/ $\alpha$ -CD-PN-film:** Cyclodextrin, either  $\beta$ - or  $\alpha$ -, (0.2 g, 1.8 mmol if  $\beta$ -CD or 2.1 mmol if  $\alpha$ -CD) was dissolved in methanesulfonic acid (2 mL) and pre-reacted for 30 min with bath sonication, forming a dark red solution. The solution was then heated for 3 h at 110°C. (Note: the reaction time should be tailored according to the volume of the reaction solution, in order to obtain a viscous yet fluid solution for casting.) After the appropriate reaction time, the solution is cooled and cast onto a glass substrate using a glass pipet. Bubbles should be removed if possible. Two pieces of micro cover glass divider with a thickness between 0.12-0.17mm are placed on either side of the substrate (**Fig. S5**). Then another piece of glass is slowly placed on top. The sandwiched system was further heated at 110°C for 48 h. Afterwards, the glass on top was carefully removed leaving the film on the bottom glass substrate. The film was subsequently washed with copious amounts of water.

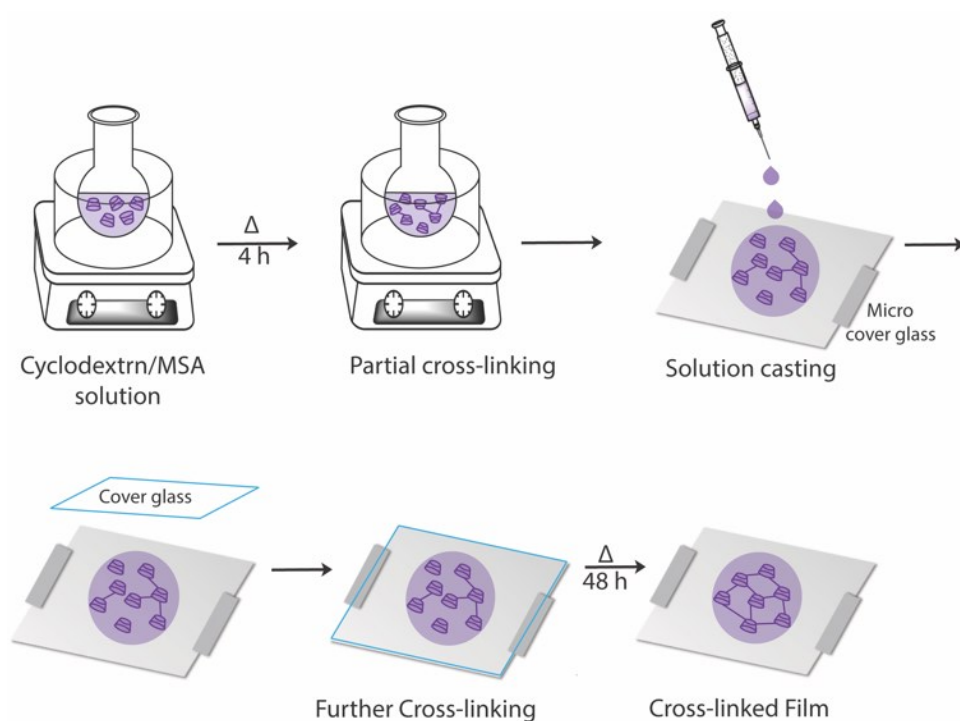


**Fig. S7** CD-PN film fabrication method.

## 9. Scanning Electron Microscopy

SEM samples were coated with 3 nm of platinum/palladium, 80% and 20%, respectively, using a Cressington Sputter Coater 208 HR for high resolution FE-SEM coating to make the samples conductive. SEM images of the  $\beta$ -CD-PN sample powderized by a commercial coffee grinder and the thin films as described in **Section 7** were recorded.

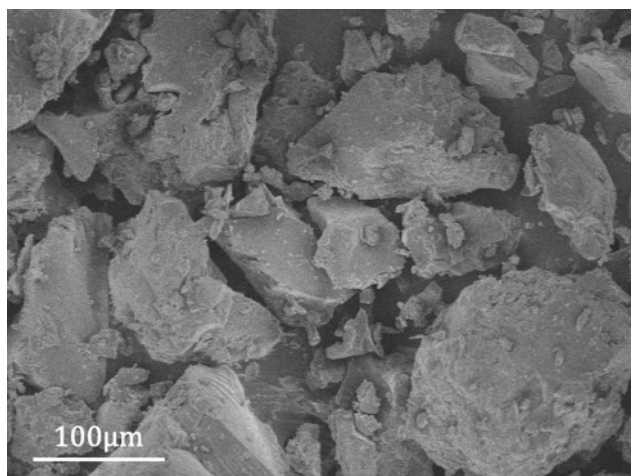


**Fig. S8** SEM image of  $\beta$ -CD-PN sample powdered by a commercial coffee grinder.

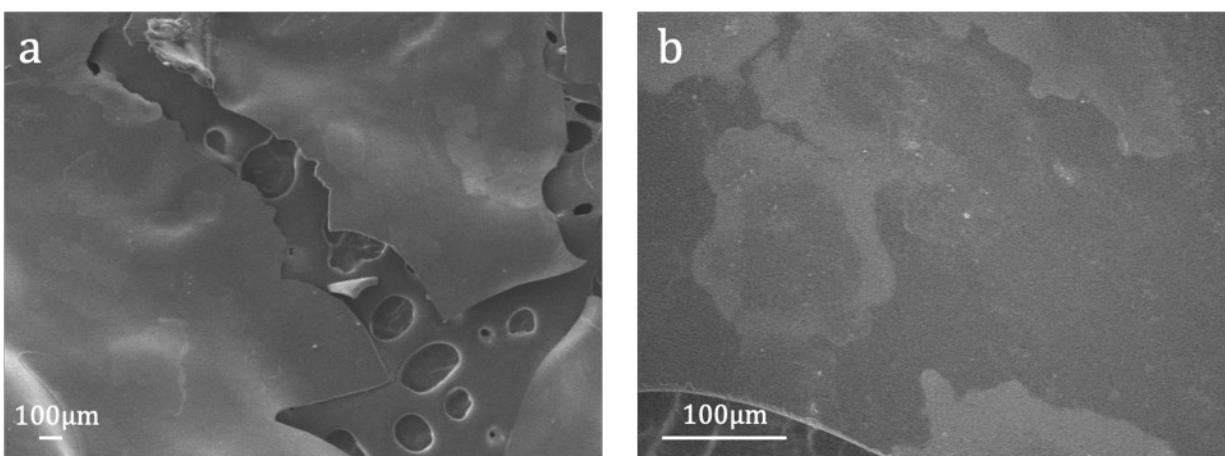


**Fig. S9** The top view SEM images of  $\beta$ -CD-PN film.

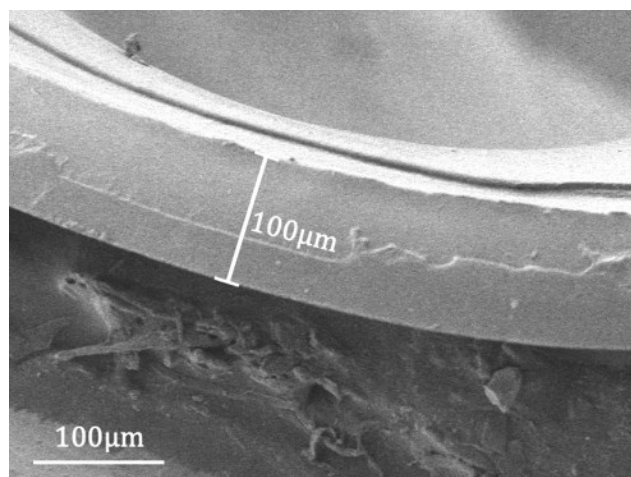


**Fig. S10** The cross-section view SEM image of  $\beta$ -CD-PN film.

## 10. Structure Size Modeling

The molecular structures of the dyes were modeled using ChemDraw3D. The molecule sizes were measured on ChemDraw3D between particular atoms within the molecule to give a general idea of the molecular dimensions. These measurements were validated by comparing some of these data with single crystal structures from Cambridge Crystallographic Data Centre analyzed with Mercury crystallography analysis software, which showed percent difference between 0.4~8.5%.

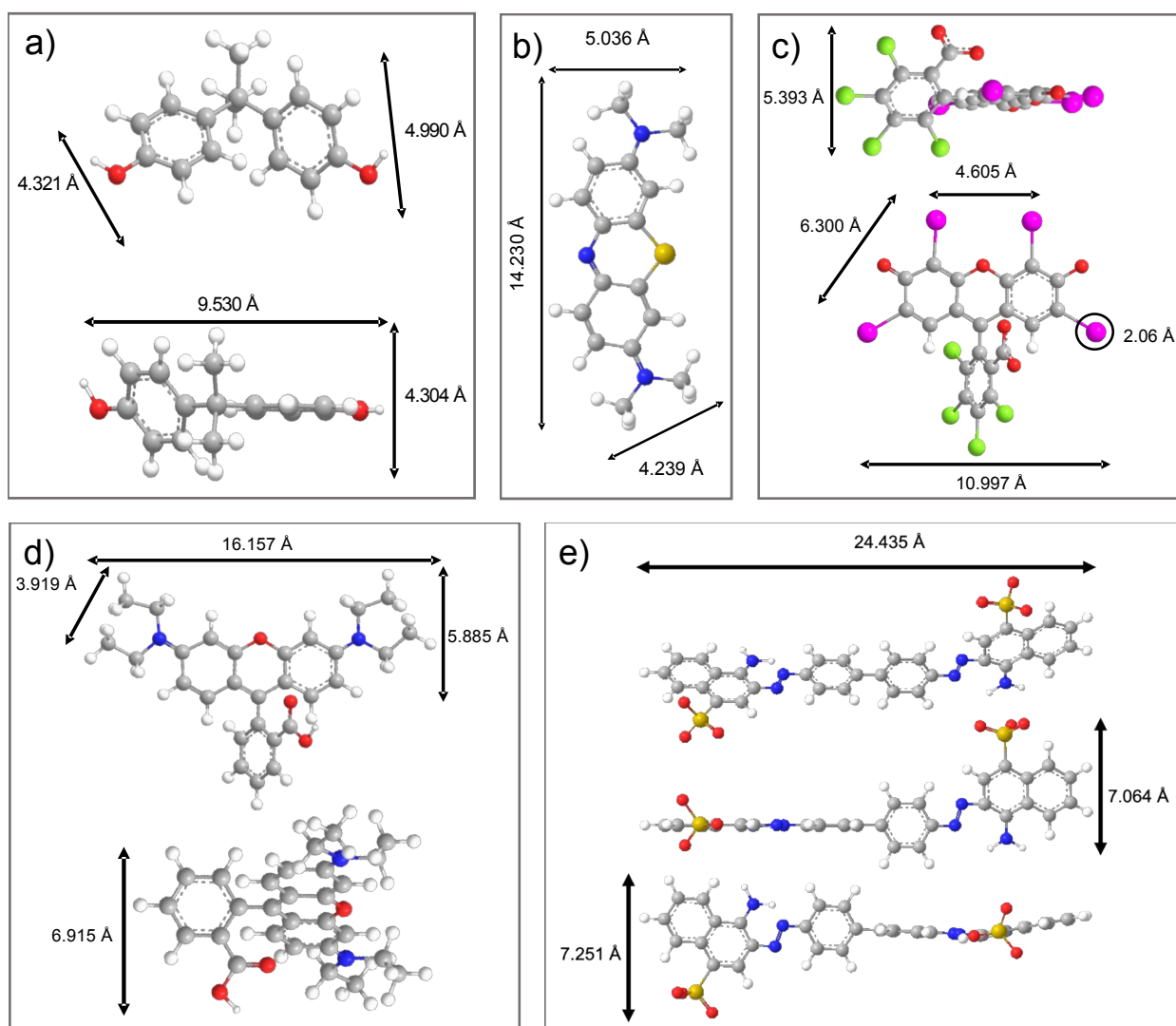


**Fig. S11** Molecular structures and dimensions of the dyes tested in the study. (a) bisphenol A, (b) methylene blue, (c) rose bengal, (d) rhodamine B, and (e) congo red.

## 11. Adsorption Performance

### 11.1 Adsorption Rate

Powder of  $\beta$ -CD-PN (12 mg) was added into an aqueous solution of organic compounds (12 mL, 0.1 mM). As the solution was stirred, 2 mL aliquots were removed at the time intervals of 10 seconds, 30 seconds, 1 minute, 2 minutes, 5 minutes, and 10 minutes, respectively. The aliquots were passed through a syringe filter to remove the solid CD-PN. The adsorption efficiency was determined by comparing the UV-vis absorbance of these sample with that of the initial solution (*Equation S3*), where  $C$  = sample concentration and  $C_0$  = initial concentration. The organic compounds tested were methylene blue, bisphenol A, rose Bengal, rhodamine B, and Congo red. The  $\beta$ -CD-PN demonstrated fast and selective adsorption of smaller organic molecules, *i.e.*, methylene blue and bisphenol A, within 10 minutes. Adsorption efficiencies of all the other larger organic molecules were lower than 10% after 10 minutes.

$$\text{Adsorption Efficiency (\%)} = \left(1 - \frac{C}{C_0}\right) \times 100 \quad (\text{Equation S3})$$

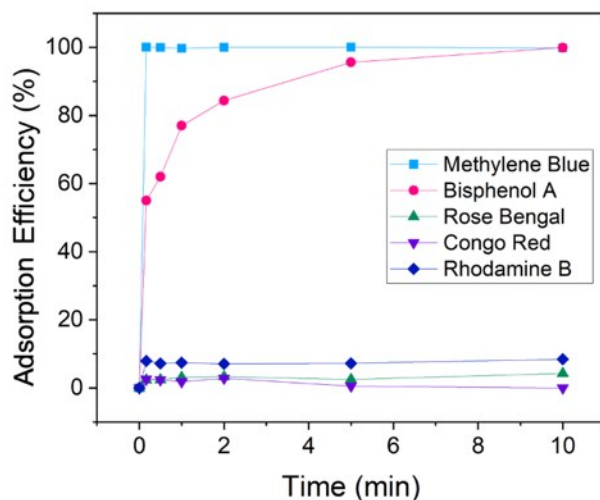


**Fig. S12** Adsorption efficiency of different organic molecules by  $\beta$ -CD-PN as a function of time.

### 11.2 $\beta$ -CD-PN Film Solution Adsorption

$\beta$ -CD-PN film pieces (15 mg) were added into an aqueous solution of organic compounds (15 mL, 0.1 mM). The solution was stirred for 30 minutes, and then a sample was passed through a syringe filter to remove any small pieces of film that broke off during the stirring. The removal efficiency of the  $\beta$ -CD-PN film was determined as described in **Section 11.1**. The organic compounds tested were methylene blue, bisphenol A, rose Bengal, rhodamine B, and Congo red. The selectivity is maintained in the film with bisphenol A and methylene blue being adsorbed, while larger molecules are adsorbed to a much lesser amount. Although the selectivity is still observed, the larger dye molecules were adsorbed more so to the film than was observed for the bulk powder (**Fig. S13**). It is believed that this is a result of physical adsorption to the film surface rather than into the pores derived from  $\beta$ -cyclodextrin.

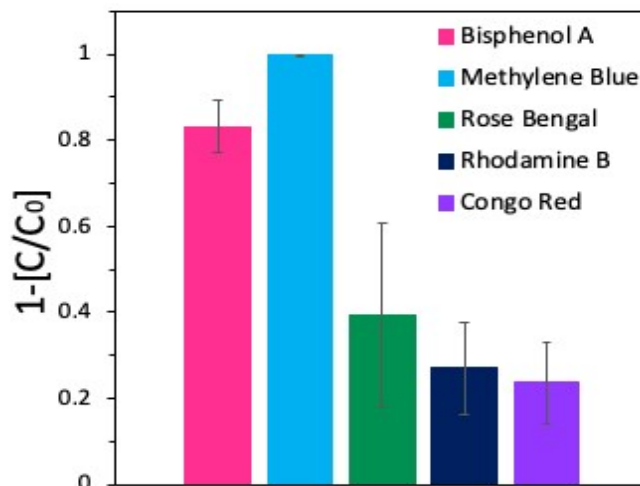


**Fig. S13** Adsorption efficiency of different organic molecules by  $\beta$ -CD-PN. The adsorption efficiency is an average of 4 trials.

### 11.3 Adsorption Isotherm

The adsorption isotherms were obtained by adding  $\beta$ -CD-PN (15 mg) to either a methylene blue or bisphenol A solution in water (20 mL) and stirred for 24 h. UV-visible absorption spectra of the solution were recorded to monitor concentration before and after adsorption. The initial concentrations of the solutions were varied from 0.05 to 2.0 mM. The adsorption isotherms were fitted using the Langmuir-Freundlich adsorption isotherm (*Equation S4*), where  $Q_e$  (mg/g) is the amount of dye adsorbed at equilibrium,  $C_e$  (mg/g) is the equilibrium solute concentration,  $Q_{max}$  (mg/g) is the maximum adsorption capacity,  $b$  is the Langmuir equilibrium constant, and  $n$  is the Freundlich heterogeneity index.<sup>1</sup> The Langmuir-Freundlich isotherm was chosen to characterize the isotherms because it is applicable to both homogeneous and heterogeneous materials, while also describing the adsorption capacity. The CD-PN materials are expected to have a certain level of heterogeneity due to the myriad of reactions that can occur during synthesis (*e.g.*, ring-opening,  $\beta$ -elimination) leading the Langmuir-Freundlich isotherm to be a better fit than the Langmuir isotherm.

$$Q_e = \frac{Q_{max} b C_e^{1-n}}{1 + b C_e^{1-n}} \quad (\text{Equation S4})$$

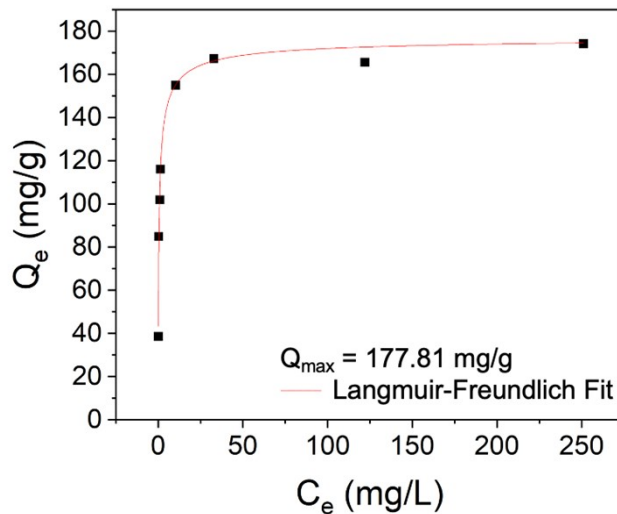


**Fig. S14** Isotherm corresponding to the adsorption of methylene blue on  $\beta$ -CD-PN ( $R^2 = 0.9907$ ).

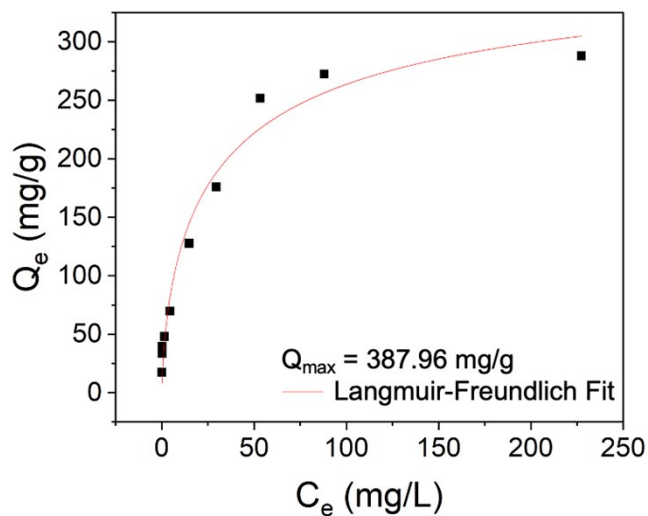


**Fig. S15** Isotherm corresponding to the adsorption of bisphenol A on  $\beta$ -CD-PN ( $R^2 = 0.9609$ ).

#### 11.4 Column Adsorption

An adsorption column was prepared in a syringe (1 mL) by placing a small piece of cotton at the bottom, followed by adding ~100 mg of  $\alpha$ - $\beta$ -CD-PN, Glu-PN, or activated carbon as the

stationary phase. An aqueous dye solution (0.2 mM) was then prepared. The solution was passed through the column driven by pressurized air with a flow rate of approximately ~0.4 mL/s and an empty bed contact time of approximately ~0.5 seconds. The eluent was collected as fractionated samples (3.5 mL each). The dye concentration in each eluent sample was determined using UV-visible absorption spectroscopy. The amount of dye adsorbed was then calculated based on the concentration difference between the stock solution and eluent. The samples for methylene blue, Congo red, and rose Bengal were diluted before the absorbance measurement in order to fulfill the Beer-Lambert law.

### **11.5 Column Adsorption with Interference**

A column was prepared as described above using  $\beta$ -CD-PN. A mixed rhodamine B and methylene blue solution in water was prepared (0.1 mM rhodamine B + 0.005 mM methylene blue). The mixed solution was passed through the columns as described in **Section 11.4**. The eluent was collected and measured with UV-visible absorption spectroscopy as described above.

### **11.6 Recyclability**

$\beta$ -CD-PN (20 mg), either virgin or recycled, was stirred in a solution of methylene blue (20 mL, 0.1 mM) for 1 h. The amount of adsorbed methylene blue was determined by comparing the light absorbance of the solution before and after  $\beta$ -CD-PN treatment. After each test, the  $\beta$ -CD-PN was stirred in 30 mL of methanol at 35°C for 2 h to cleanse the adsorbed methylene blue, and subsequently collected via centrifugation, followed by washing and drying. The recycled sample was then dried under vacuum before use in the next cycle.

### **11.7 Solvent Resistance**

$\beta$ -CD-PN (100 mg) was suspended and stirred in each of the following solvent/solution for 1 week: 0.1 M HCl, 0.1 M NaOH, Methanol, dichloromethane, hexanes, or acetone. Afterwards, the

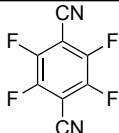
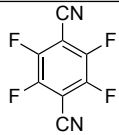
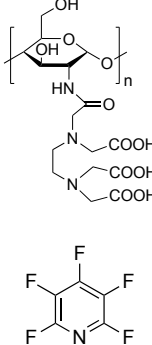
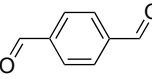
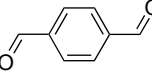
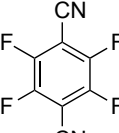
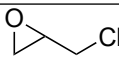
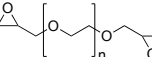
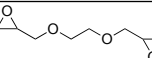
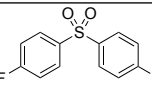
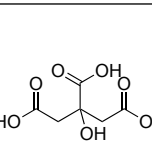
suspended solid was collected by centrifugation, washed, and dried under vacuum. Materials soaked in HCl or NaOH solutions were washed thoroughly with water before drying. After drying, the treated  $\beta$ -CD-PN (12 mg) was added into a methylene blue solution (12 mL, 0.1 mM) and stirred for 24 h. The methylene blue adsorption amount was then measured by UV-visible absorbance before and after the treatment.

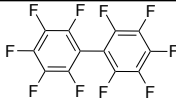
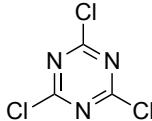
## 12. Cyclodextrin-Based Polymer Comparison

The structure, synthetic conditions, and BPA adsorption capacity are compared for a series of cyclodextrin-based polymers. The prime difference between the  $\beta$ -CD-PN polymer reported in this work and other cyclodextrin based polymers is that it is linker-less, meaning the cyclodextrin is directly crosslinked with no additional crosslinker. Additionally, the synthetic conditions are considerably greener than many of the other cyclodextrin-based polymers. The BPA adsorption capacity of  $\beta$ -CD-PN is significantly higher than other cyclodextrin-based polymers. This comparison supports the theory that the linker-less CD-PN polymer has the potential for an enhanced binding site density, which enables it with a high adsorption capacity from cyclodextrin itself. Although this parameter gives a general idea of adsorption performance, it is prudent to mention that varying techniques and measurement methods could cause some discrepancy between the reported values.

**Table S3.** Comparison of crosslinked cyclodextrin-based polymers.

Polymer	Monomer	Crosslinker	Conditions	CD Functionalization	BPA $Q_{\max}$ (mg/g)	Citation
CD-PN	$\beta$ -CD	N/A	MSA, 110°C, 48 h	Dehydrated	388	This Work

P-CDP	$\beta$ -CD		$K_2CO_3$ , THF, 80 °C, 48 h	N/A	88	Alsbaiee <sup>2</sup>
TFN-CDP-2	$\beta$ -CD		$K_2CO_3$ , DMSO, 80 °C, 18 h	Phenolated	250	Klemes <sup>3</sup>
P-CDEC	$\beta$ -CD		8:1 MeTHF:H <sub>2</sub> O, $K_2CO_3$ , 80 °C, 48 h	N/A	59-66*	Yu <sup>4</sup>
$\beta$ -CD COF	heptakis(6-amino-6-deoxy)- $\beta$ -CD		50:50 EtOH:H <sub>2</sub> O, AcOH, r.t., 48 h	Aminated	20	Wang <sup>5</sup>
$\beta$ -CD NCP	heptakis(6-amino-6-deoxy)- $\beta$ -CD		50:50 EtOH:H <sub>2</sub> O, Ammonia, r.t., 48 h	Aminated	10	Wang <sup>5</sup>
P-CD-P5A-P	$\beta$ -CD, Pillar[5]arene		$K_2CO_3$ , THF, 80 °C, 72 h	N/A	258	Lu <sup>6</sup>
T-E-CDP	$\beta$ -CD		NaOH <sub>(aq)</sub> , 90°C, 3 h	N/A	128*	Xu <sup>7</sup>
ECP	$\beta$ -CD		NaOH	N/A	84	Morin-Crini <sup>8</sup>
PEGCDP	$\beta$ -CD		NaOH <sub>(aq)</sub> , 60°C, 5 h	N/A	71	Kono <sup>9</sup>
EGCDP	$\beta$ -CD		NaOH <sub>(aq)</sub> , 60°C, 5 h	N/A	78	Kono <sup>9</sup>
$\beta$ -CDP	$\beta$ -CD		Toluene, DMAc, $K_2CO_3$ , 150°C, 12 h	N/A	113	Wang <sup>10</sup>
CD-CA-g-PDMAEMA	$\beta$ -CD, 2-dimethylamino ethyl methacrylate (DMAEMA)		1) $KH_2PO_4$ , 140°C, 3 h 2) $K_2S_2O_8$ , 80°C, 30 min 3) 1 M HCl 4) DMAEMA, 80°C, 3 h	N/A	79	Zhou <sup>11</sup>

MP-CDP (DFP-CDP) <sup>12</sup>	$\beta$ -CD		K <sub>2</sub> CO <sub>3</sub> , 1:3 THF:DMF, 85 °C, 72 h	N/A	79	Li <sup>13</sup>
CDW7-Triazine	$\beta$ -CD		NaOH, BDMHAC, CH <sub>3</sub> CN, H <sub>2</sub> O	N/A	57	Wang <sup>14</sup>

## References

1. R. J. Umpleby, S. C. Baxter, Y. Chen, R. N. Shah and K. D. Shimizu, *Anal. Chem.*, 2001, **73**, 4584-4591.
2. A. Alsbaiee, B. J. Smith, L. L. Xiao, Y. H. Ling, D. E. Helbling and W. R. Dichtel, *Nature.*, 2016, **529**, 190-U146.
3. M. J. Klemes, Y. H. Ling, M. Chiapasco, A. Alsbaiee, D. E. Helbling and W. R. Dichtel, *Chem. Sci.*, 2018, **9**, 8883-8889.
4. T. T. Yu, Z. M. Xue, X. H. Zhao, W. J. Chen and T. C. Mu, *New J. Chem.*, 2018, **42**, 16154-16161.
5. R. Q. Wang, X. B. Wei and Y. Q. Feng, *Chem.-Eur. J.*, 2018, **24**, 10979-10983.
6. P. P. Lu, J. C. Cheng, Y. F. Li, L. Li, Q. Wang and C. Y. He, *Carbohydr. Polym.*, 2019, **216**, 149-156.
7. G. Z. Xu, X. C. Xie, L. Qin, X. J. Hu, D. L. Zhang, J. Xu, D. W. Li, X. W. Ji, Y. Huang, Y. Z. Tu, L. Jiang and D. Y. Wei, *Green Chem.*, 2019, **21**, 6062-6072.
8. N. Morin-Crini and G. Crini, *Progress in Polymer Science*, 2013, **38**, 344-368.
9. H. Kono, T. Nakamura, H. Hashimoto and Y. Shimizu, *Carbohydr. Polym.*, 2015, **128**, 11-23.
10. Z. H. Wang, P. B. Zhang, F. Hu, Y. F. Zhao and L. P. Zhu, *Carbohydr. Polym.*, 2017, **177**, 224-231.
11. Y. B. Zhou, Y. H. Hu, W. W. Huang, G. Cheng, C. Z. Cui and J. Lu, *Chemical Engineering Journal*, 2018, **341**, 47-57.
12. L. L. Xiao, Y. H. Ling, A. Alsbaiee, C. J. Li, D. E. Helbling and W. R. Dichtel, *J. Am. Chem. Soc.*, 2017, **139**, 10585-10585.
13. Y. R. Li, P. P. Lu, J. C. Cheng, X. L. Zhu, W. Guo, L. J. Liu, Q. Wang, C. Y. He and S. R. Liu, *Talanta.*, 2018, **187**, 207-215.
14. J. Wang and M. Harrison, *J. Incl. Phenom. Macro.*, 2018, **92**, 347-356.